Environ. Sci. Technol. **1998**, *32,* 584−590

Effects of Non-Equilibrium Hygroscopic Growth of $(NH_4)_2SO_4$ on Dry Deposition to Water Surfaces

MARIA J. ZUFALL,*,† MICHAEL H. BERGIN,‡,§,∥ AND CLIFF I. DAVIDSON†

Department of Civil and Environmental Engineering, Carnegie Mellon University, Pittsburgh, Pennsylvania 15213, NOAA Climate Monitoring and Diagnostics Laboratory, R/E/CG1, 325 Broadway, Boulder, Colorado 80303, Brookhaven National Laboratory, Environmental Chemistry Division, Upton, New York 11973

Growth of hygroscopic aerosols near water surfaces is believed to enhance dry deposition rates, which are a strong function of particle size. Previous dry deposition models estimate hygroscopic growth by assuming equilibrium between aerosols and water vapor (Williams, R. M. *Atmos. Environ.* **1982**, *16*, 1933−1938). A model is presented here that combines the relative humidity profile above water surfaces with hygroscopic growth rates for $(NH_4)_2SO_4$, assuming cases for a deliquescing and metastable aerosol. Model results show that particles greater than 0.1 μm in diameter do not grow to their equilibrium size before depositing to a hypothetical water surface. As a consequence, equilibrium models overpredict the effects of hygroscopic growth on deposition velocities by as much as a factor of 5. In addition, model results suggest a significant difference in the deposition velocities of metastable and deliquescing aerosols. Based on measured $(NH_4)_2SO_4$ size distributions, overall deposition velocities calculated from a thermodynamic equilibrium model, a mass transfer limited non-equilibrium model with a deliquescing aerosol, and a mass transfer limited non-equilibrium model with a metastable aerosol are 0.11, 0.055, and 0.040 cm/s, respectively.

Introduction

Dry deposition of particulate contaminants to natural waters contributes to the degradation of aquatic ecosystems. For example, excess inputs of nutrients may enhance eutrophication (*2*), and deposition of toxic species may harm aquatic life (*3*). Dry deposition can account for a major fraction of the total atmospheric deposition to natural bodies of water. Gatz (*4*) estimated that the wet and dry atmospheric inputs of several trace species to Lake Michigan were approximately equal. In addition, Wu et al. (*5*) found dry deposition responsible for approximately 80% of the total atmospheric flux of Al and Fe, 50% of total atmospheric flux of As, Cr, Cu, and Ni, and 40% of the total atmospheric flux for Mn, Pb, and Zn to the Chesapeake Bay.

* Corresponding author phone: 412-268-5811; fax: 412-268-7813; e-mail: mz25@andrew.cmu.edu.

† Carnegie Mellon University.

‡ NOAA Climate Monitoring and Diagnostics Laboratory.

§ Brookhaven National Laboratory.

∥ Present address: University of Colorado, Cooperative Institute for Research in Environmental Sciences, Boulder, CO 80309.

The mass flux of aerosol particles to a body of water depends on the mass concentration and deposition velocity of the particles. The deposition velocity for an aerosol chemical species ranges over several orders of magnitude and is primarily a function of the particle size distribution (*6*), but also depends on several other factors including meteorology, surface roughness, and aerosol chemical composition. According to the model of Williams (*1*), the deposition velocity of small particles (<0.5 μm) varies approximately according to $d_p^{-0.8}$, and the deposition velocity of large particles (>1 μm) is a function of d_p^2. Due to this particle size dependence, the deposition velocity of a hygroscopic aerosol may significantly change as the particles grow.

High humidity near the water surface leads to growth of hygroscopic particles (*7*). Estimates suggest that roughly 60% of aerosol mass is hygroscopic and consists primarily of inorganic salts and organic species (*8*). The effects of hygroscopic growth are most pronounced over freshwater, where the relative humidity may approach 100%. Over saltwater, the relative humidity is limited to approximately 98.3% due to Raoult's law.

Currently, the model of Williams (*1*) or of Slinn and Slinn (*9, 10*) is used to predict dry deposition to natural water surfaces. These models divide the atmosphere into two separate layers: the free atmosphere, which extends from the viscous sublayer to any reference height, and a small (<1 cm) quasi-laminar flow region immediately above the water surface where the flow is dominated by viscous forces. In the free atmosphere, these models assume that hygroscopic growth is negligible. In the viscous sublayer, the models assume that the particles instantaneously obtain their equilibrium size. The new particle size is determined from the equilibrium model of Fletcher (*11*) using the approximations of Fitzgerald (*7*). The relative humidity in the viscous sublayer is assumed to be either 99% or 100%. Growth is assumed to occur according to

$$d_{pw} = 4.5 d_{pd}^{1.04} \qquad \text{RH} = 99\%$$

$$d_{pw} = 23 d_{pd}^{1.5} \qquad \text{RH} = 100\%$$

where d_{pd} and d_{pw} are the particle diameters before and after growth, respectively.

These dry deposition models are used in conjunction with measured airborne concentrations of specific pollutants to estimate dry deposition to bodies of water. For example, Dulac et al. (*12*) used the Williams model to estimate the flux of mineral aerosol particles to the North Sea, and Lindfors et al. (*13*) used this model to estimate deposition fluxes of sulfur and nitrogen to the Baltic Sea. Since it is difficult to experimentally measure dry deposition fluxes to water surfaces (*14*), measured concentrations and modeled deposition velocities are often the only means of estimating dry deposition fluxes of pollutants to bodies of water.

The effects of hygroscopic growth on the dry deposition velocity according to the Williams (*1*) model are shown in Figure 1. The two curves at 99% and 100% relative humidity in the viscous sublayer show a significant increase in deposition velocity of particles in the accumulation mode size range ($d_p \sim 0.1-1$ μm) as compared to the no growth case. In general, a considerable mass fraction of anthropogenic atmospheric pollutants exists in this size range (*15*). The deposition velocity increases by factors of 10 and 19 for 1-μm particles at 99% and 100% relative humidity, respec-

S0013-936X(97)00476-8 CCC: $15.00
Published on Web 01/22/1998

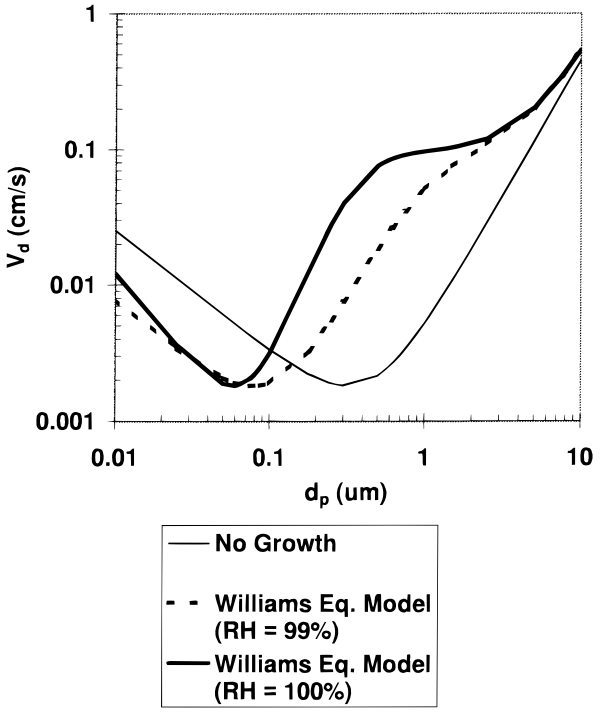

FIGURE 1. Dry deposition velocity as predicted by the Williams (*1*) model for a wind speed of 2 m/s and a stable atmosphere. The effects of hygroscopic growth on deposition velocity are illustrated by the change in V_d with different relative humidities in the viscous sublayer, shown in parentheses.

tively, and decreases by a factor of 3 for 0.05-μm particles at both 99% and 100% relative humidity.

Particles larger than 1 μm in diameter are deposited mainly by gravity. As size (and therefore mass) increases, the gravitational force becomes stronger and the deposition velocity increases. Particles less than 0.1 μm in diameter are predominantly influenced by Brownian diffusion, which decreases with increasing particle size. Particles in the range of approximately 0.1−1 μm in diameter are not strongly affected by either of these mechanisms. Hygroscopic growth of particles greater than a few tenths of a micrometer in diameter leads to an increase in deposition velocity as these particles are increasingly influenced by gravity. The opposite occurs for small (<0.1 μm) particles because the influence of Brownian diffusion is diminished.

In this paper, a new model is developed to predict the dry deposition velocity of hygroscopic particles [$(NH_4)_2SO_4$] to water surfaces. The model does not assume equilibrium between aerosols and water vapor but rather considers detailed water vapor mass transport. In addition, this paper considers the possibility of the presence of both crystalline solid particles and metastable aqueous droplets. $(NH_4)_2SO_4$ was chosen due to the available thermodynamic data, its prevalence in the atmosphere, and its nonreactive nature. The results for $(NH_4)_2SO_4$ provide insight into the effects of hygroscopic growth on other aerosol species of interest.

Model Development

Relative Humidity Profile. The relative humidity profile calculations used in this model are taken from Roll (*16*) and Avery (*17*). The relative humidity profile may be determined from the flux of moisture away from the water surface:

$$\frac{dq}{dz} = \frac{-E}{\rho K_e} \tag{1}$$

where q is the specific humidity of air, E is the eddy flux of moisture, ρ is the density of air, and K_e is the eddy transfer coefficient of moisture. It is assumed that K_e is equal to the eddy viscosity of air, K_m (*18*). The latter variable is defined as

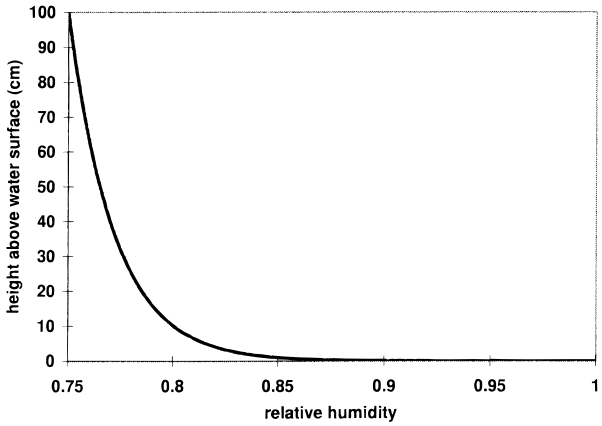

FIGURE 2. Relative humidity profile based on Avery (*17*) for a 75% relative humidity at a height of 1 m over a water surface.

$$K_m = ku_*z \tag{2}$$

where k is von Karman's constant, u_* is the friction velocity, and z is the height above the surface.

The eddy flux of moisture is determined according to Montgomery (*19*):

$$E = \frac{\rho k(q_o - q_a)u_*}{(\alpha\nu k/D) + \ln(ku_*a/D)} \tag{3}$$

where q_o is the relative humidity at the surface (assumed to be 100%), q_a is the relative humidity at height a, α is a dimensionless constant equal to 5, ν is the kinematic viscosity of air, and D is the diffusivity of water vapor in air. Figure 2 shows the relative humidity profile above a water surface for initial conditions of 75% humidity at 1 m above the water surface.

Hygroscopic growth occurs mainly in the lowest several centimeters near the water surface. Unfortunately, there are no measurements of the relative humidity near water surfaces, preventing verification of the model.

Hygroscopic Growth. The rate of particle growth due to water vapor condensation depends on several factors including relative humidity, water vapor pressure above the particle surface, and mass transport regime. Far from the particle surface, water vapor transport occurs by diffusion due to a concentration gradient. Closer to the particle surface, the velocity distribution becomes anisotropic, and there is a component of the velocity of water vapor molecules that is directed toward the particle surface. The diffusion flux of vapor is superimposed with the directed flux at the surface to develop the equation for water vapor flux to a particle (*20*). This formulation is further modified by including the accommodation coefficient to account for molecules that collide with a particle but do not condense. The accommodation coefficient represents the fraction of water molecules that condense on to the particle after a collision. These processes are described in terms of particle growth by the following equation (*21*):

$$\frac{dd_p}{dt} = \frac{4D_wF(Kn)A(C_w - C_s)}{\rho_p d_p} \tag{4}$$

where d_p is the particle diameter, t is the time, D_w is the water vapor diffusivity, ρ_p is the particle density, C_w is the water

vapor concentration in the ambient air, C_s is the water vapor concentration at the particle surface, and $F(K_n)$ and A are defined as follows (*21*):

$$Kn = 2\lambda/d_p \quad (5)$$

$$F(Kn) = (1 + Kn)/(1 + 1.71Kn + 1.33Kn^2) \quad (6)$$

$$A = 1/(1 + 1.33KnF(Kn)(1/A_o - 1)) \quad (7)$$

where λ is the mean free path of air molecules = 0.065 μm and A_o is the accommodation coefficient, assumed to be equal to 0.1.

Water Vapor Concentration Calculations. C_w and C_s are calculated from the water vapor pressure and the ideal gas law. The water vapor pressure far from the particle surface is defined as the saturation water vapor pressure multiplied by the relative humidity. The saturation vapor pressure over water is determined for a given temperature from Lowe and Ficke (*22*).

If a particle is in equilibrium with its environment, the water vapor pressure near the particle P_s is equal to the ambient water vapor pressure P_w. However, in the viscous sublayer, a steep humidity gradient exists and equilibrium may not be reached. The difference between the vapor pressures in the air and at the particle surface provides the concentration gradient for water vapor diffusion and thus the driving force for particle growth.

The vapor pressure at the particle surface depends on the effects of particle curvature and solute concentration (*8*). The curvature of the particle surface leads to the Kelvin effect, which states that the vapor pressure around a curved surface is greater than the vapor pressure over a flat surface. The effect of curvature on water vapor pressure can be quantified as (*23*):

$$P_{Ks} = P_w \exp\left(\frac{4M_w\sigma}{RT\rho_w d_p}\right) \quad (8)$$

where P_{Ks} is the vapor pressure at the particle surface due to Kelvin effects, M_w is the molecular weight of water, σ is the surface tension, R is the universal gas constant, T is the temperature, and ρ_w is the density of water.

The presence of a solute reduces the water vapor pressure around the particle because the solute has no water vapor pressure of its own. The water vapor pressure around a specific salt at known concentration, temperature, and pressure can be predicted from thermodynamic theory. Models based on the Gibbs−Duhem equation developed for an aqueous solution containing dissolved $(NH_4)_2SO_4$ (*24*) compare to experimental data within 8% (*25*). Empirical fitting of the thermodynamic model of Kusik and Meissner (*24*) gives the following equation for water vapor pressure as a function of mass fraction of solute mfs (*25*):

$$P_{Ss} = P_w(0.99 - 0.295\text{mfs} - 0.114\text{mfs}^2 + 1.56\text{mfs}^3 - 8.18\text{mfs}^4 + 6.98\text{mfs}^5) \quad (9)$$

where P_{Ss} is the vapor pressure due to solute effects. This equation is valid for solute mass fractions less than 0.7. For solute mass fractions greater than 0.7, experimental results show that the ratio of P_{Ss} to P_w is approximately 0.47. The effects of curvature and solute concentration on water vapor pressure are combined to give the water vapor pressure around the particle:

$$P_s = \left(\frac{P_{Ks}P_{Ss}}{P_w}\right) \quad (10)$$

Deliquescence and Metastable Particles. Particle growth does not begin until the relative humidity reaches the deliquescence humidity for that species [80.2% for $(NH_4)_2SO_4$ at 20 °C (*26*)]. Prior to deliquescence, particles exist in a crystalline solid phase, and afterwards they exist as solution droplets. However, due to changes in relative humidity during transport, a particle may deliquesce and then move into a lower relative humidity region. Since particles recrystallize at lower humidity than their deliquescence humidity [36% for $(NH_4)_2SO_4$ (*27*)], this may leave the particle in a metastable state, existing as a supersaturated solution droplet below its deliquescence humidity (*28*).

Recent studies at the Grand Canyon, Mojave Desert, and Riverside, CA, found that metastable particles existed more than 50% of the time when the relative humidity was between 45 and 75% (*28*). This prevalence of metastable particles can have significant effects on hygroscopic growth and dry deposition velocity predictions. With respect to hygroscopic growth, metastable particles act differently from solid particles in two ways. First, since metastable solution droplets have already deliquesced, they will uptake water at a relative humidity below their deliquescence humidity. Second, these particles will exhibit a less significant size change because they already contain a fraction of water.

Model Structure. To estimate the dry deposition velocity of $(NH_4)_2SO_4$ particles, several initial conditions must be specified including the initial particle size distribution, aerosol chemical composition, relative humidity, and height above the water surface. The particle is considered to be initially in one of two states: dry or metastable. An initially dry particle does not begin to grow until the relative humidity reaches the deliquescence point. Once the deliquescence point is reached, the particle will begin to grow according to the mass transport equation (eq 4).

Metastable particles uptake water when the relative humidity increases starting at a relative humidity below their deliquescence point. In this model, metastable particles are initially assumed to be in equilibrium with the ambient relative humidity, regardless of their deliquescence humidity.

Once initial conditions are set, the particle moves toward the surface at its deposition velocity. The deposition velocity calculation is based on the model of Williams (*1*), which assumes steady-state conditions. For simplicity, the model is run under stable atmospheric conditions with calm water surfaces. Since unstable and rough water surface conditions enhance deposition rates, the importance of non-equilibrium effects will be more pronounced as the particles will move more quickly through the high humidity regions.

Particle growth begins as the particle moves through the relative humidity gradient. The model predicts the particle transport through the atmosphere in time steps of 0.1 s for a given initial particle size. For each time step a particle size is estimated from eq 4 based on the relative humidity at that height above the water surface and vapor pressure above the particle surface. The particle size is used to estimate the dry deposition velocity for the next time increment. This process continues until the particle reaches the water surface. The overall deposition velocity is then calculated based on the time required for a particle to move from a height of 1 m to the water surface.

Results and Discussion

Particle Growth and Deposition Velocity. The time scales for 0.01-, 0.1-, and 1-μm particles to reach equilibrium with respect to particle diameter estimated from eq 4 at 99% relative humidity are on the order of seconds, minutes, and hours, respectively. The increase in the equilibrium time scale from 0.01 to 1.0 μm particles suggests that larger particles may not reach their equilibrium size.

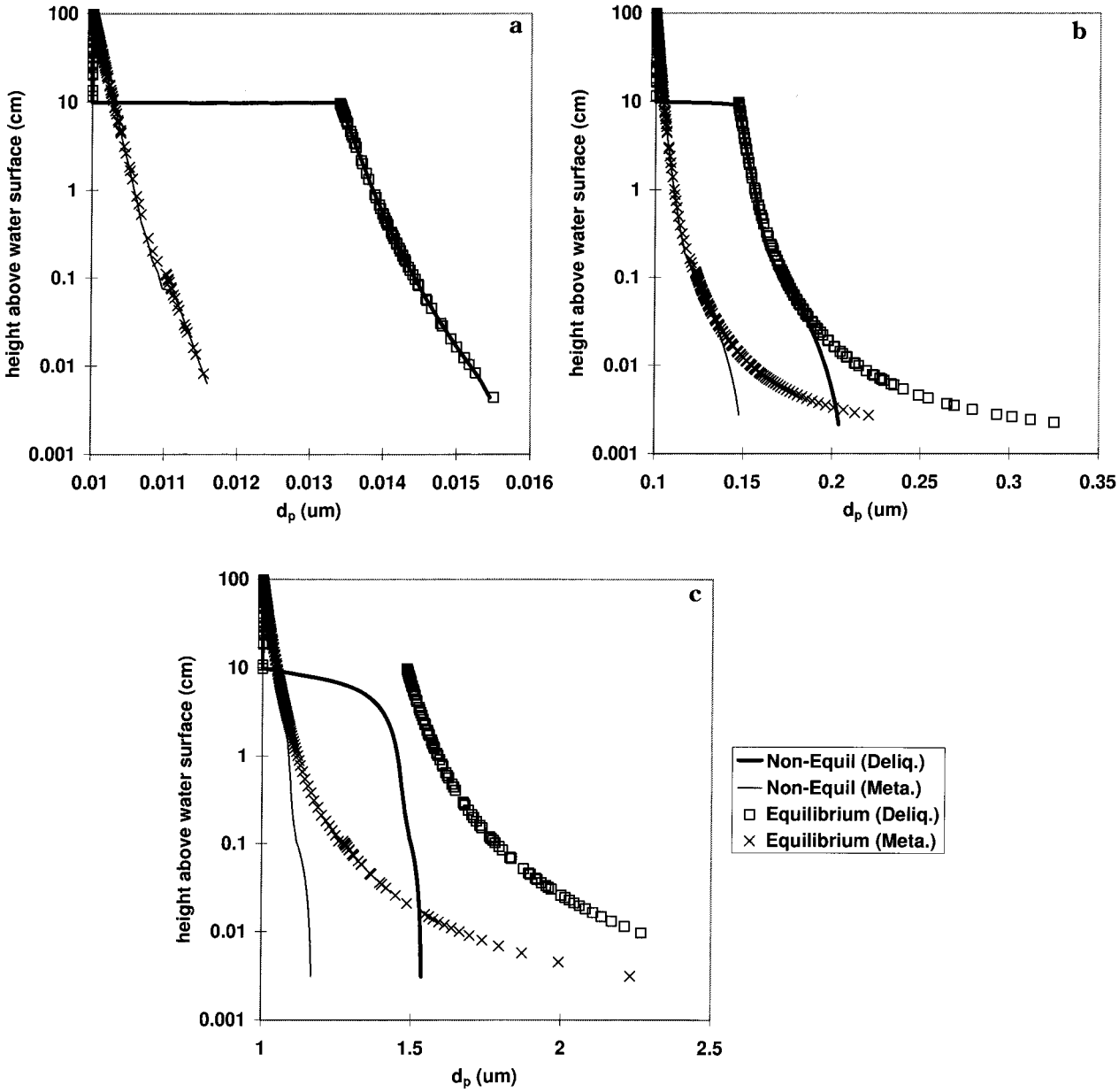

FIGURE 3. Hygroscopic growth of $(NH_4)_2SO_4$ particles with an initial diameter of (a) 0.01, (b) 0.1, and (c) 1 μm. Results are shown for growth under non-equilibrium (deliquescing), non-equilibrium (metastable), equilibrium (deliquescing), and equilibrium (metastable) conditions. The model was run under the following conditions: wind speed = 2 m/s, friction velocity = 0.063 m/s, air and water temperature = 20 °C, relative humidity at 1 m = 75% and initial height = 1 m.

Model results show significantly less growth than that predicted by assuming equilibrium based on Chan et al. (*25*). Figure 3a−c shows the growth curves for thermodynamic equilibrium and mass transfer limited non-equilibrium cases for both deliquescing and metastable aerosols as a function of height for 0.01-, 0.1-, and 1-μm $(NH_4)_2SO_4$ particles, respectively. It is apparent that particles initially greater than 0.1 μm do not grow to their equilibrium size during the time frame of deposition from a height of 1 m.

The change in particle size of metastable particles is less than that of initially dry particles because metastable particles already consist of both solute and water. This is an important consideration when estimating dry deposition flux based on size-segregated airborne concentration measurements and modeled deposition velocities.

The influence of hygroscopic growth on dry deposition rates is less than previously expected due to lower amounts of growth compared with the assumption of thermodynamic equilibrium. Figure 4 shows the deposition velocities as predicted by this model for solid (deliquescing) and aqueous (metastable) particles and the Williams equilibrium model (*1*) for 99% relative humidity and no growth. The deposition velocity curve for non-equilibrium metastable aerosols differs only slightly from the no growth case. This suggests that hygroscopic growth is a relatively unimportant consideration when determining deposition velocities of metastable aerosols. Deposition rates of initially solid particles are clearly influenced by the effects of hygroscopic growth. However, these effects are significantly less than predicted by equilibrium models.

These results are consistent with an experimental study by Jenkin (*29*) in which dry deposition rates of NaCl particles 1.25−4.2 μm in diameter were measured to wet and dry surfaces in a wind tunnel. The deposition velocity to wet surfaces was up to a factor of 2 greater than to dry surfaces.

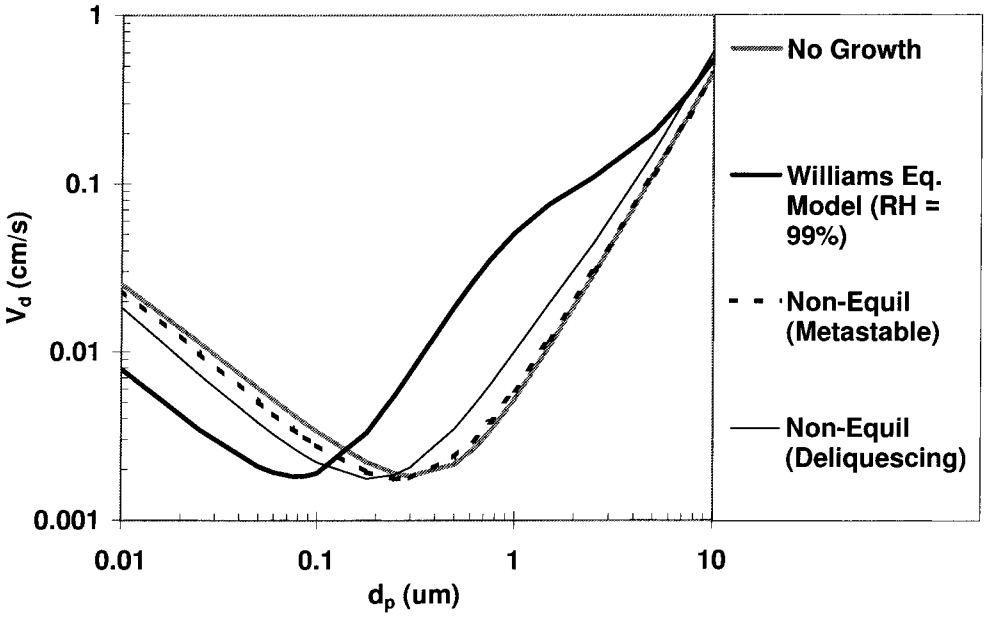

FIGURE 4. Dry deposition velocity curves for no growth, equilibrium growth (relative humidity = 99%), non-equilibrium growth (metastable), and non-equilibrium (deliquescing). Results are shown for the same conditions as Figure 3.

However, order of magnitude increases would be expected for equilibrium growth (*29*).

Implications for Deposition Estimates. It is clear from these results that non-equilibrium hygroscopic growth plays an important role in dry deposition estimates for hygroscopic aerosols. To determine the likely effects on actual $(NH_4)_2SO_4$ deposition predictions, an SO_4^{2-} airborne size distribution measured by John et al. (*30*) with Berner cascade impactors was used to determine an overall deposition velocity for an actual ambient aerosol measured in southern California. This size distribution is similar to other measured marine sulfate size distributions (*31*). In this study, measurements of sulfate and nitrate ion equivalents were nearly balanced by ammonium ions, suggesting that most of the sulfate was present as $(NH_4)_2SO_4$.

John et al. (*30*) found SO_4^{2-} to exist in 3 modes, at 0.2, 0.7, and 4.4 μm aerodynamic diameter. Log-normal distributions based on these means and geometric standard deviations of 1.5, 1.7, and 1.9, respectively, were used to generate 20 particle sizes from each mode to calculate the overall deposition velocity according to (*32*)

$$V_d = \frac{\int_{d_{p,max}}^{d_{p,min}} v_d(d_p) m(d_p)\, dd_p}{\int_{d_{p,max}}^{d_{p,min}} m(d_p)\, dd_p} \qquad (11)$$

where $v_d(d_p)$ is the deposition velocity as a function of particle diameter, and $m(d_p)$ is the mass concentration distribution function. The mass fraction in each size interval is 0.15, 0.72, and 0.13 for the 0.2, 0.7, and 4.4 μm modes, respectively (*30*).

The individual deposition velocities for each mode and condition are listed in Table 1. Based on the values in Table 1, the overall deposition velocities for $(NH_4)_2SO_4$ are 0.055 and 0.040 cm/s under mass transfer limited non-equilibrium growth of deliquescing and metastable particles, respectively. These values are a factor of 2 and 2.7 lower than predicted with equilibrium growth. It thus becomes clear that it is necessary to use hygroscopic growth under non-equilibrium conditions and to consider the presence of metastable particles in order to obtain a more accurate estimate of dry deposition velocity.

TABLE 1. Deposition Velocities for Three Log-Normal Distributions with Indicated Mean, Geometric Standard Deviation and Conditions

		deposition velocity (cm/s)		
			mass transfer limited non-equilibrium growth model	
d_p (μm)	σ_g (μm)	thermodynamic equilibrium model	solid particles	metastable particles
0.2	1.5	0.0020	0.0020	0.0024
0.7	1.7	0.0044	0.0038	0.0025
4.4	1.9	0.10	0.073	0.052

Reason for Differences. The calculations of Figures 3 and 4 incorporate three major changes from the work of Williams (*1*). First, a more realistic humidity profile based on Avery (*17*) has been used as input for the hygroscopic growth computations. Second, the model of particulate growth used here considers the effects of mass transfer rates. Finally, the presence of metastable particles is considered. To examine the effects of each change separately, deposition velocities were calculated for different model simulations. The results of these calculations are shown in Figure 5 and discussed below.

Curve B in Figure 5 shows that the inclusion of the Avery (*17*) relative humidity profile leads to a decrease from previous deposition velocity predictions (curve A) by up to a factor of 4.5. Curve C in Figure 5 shows that the introduction of mass transfer limited growth (but not the Avery (*17*) humidity profile) leads to a reduction of deposition velocity by up to a factor of 7. Taken together, these two effects produce curve D, the combined effects of the new humidity profile and the non-equilibrium growth. The proximity of these three curves suggest that both the relative humidity profile and the mass transfer limitations are important in determining the impact of hygroscopic growth on dry deposition of particles to natural water surfaces. The metastable case has not been presented here since, as previously discussed, it is not significantly different than the no growth case.

Sensitivity Analysis. Deposition velocity calculations depend on input and model parameters. This section examines the sensitivity of model results to the values of

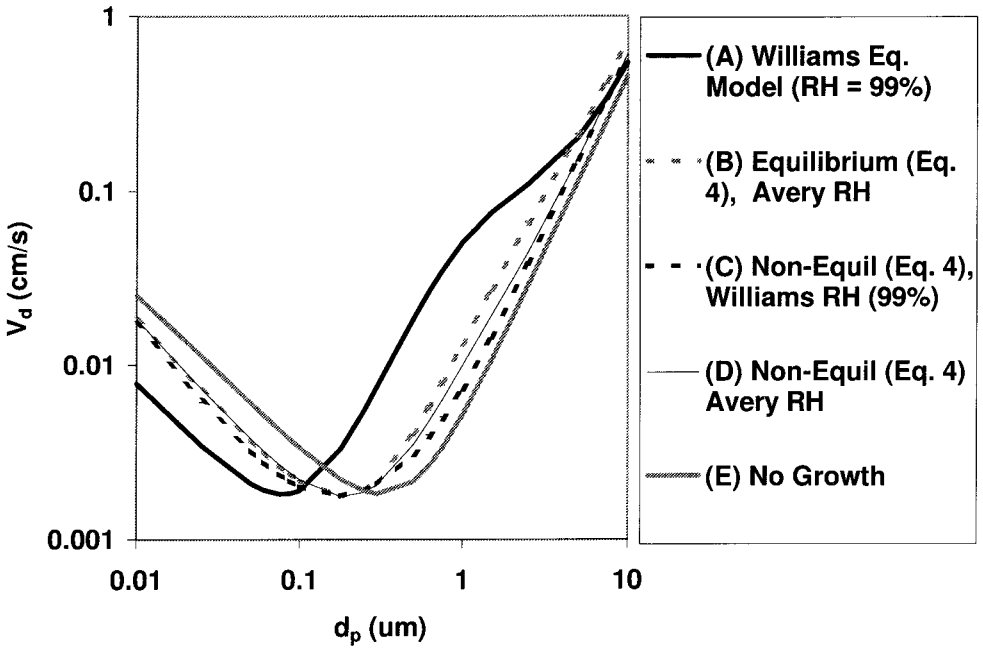

FIGURE 5. Dry deposition velocity curves for the following sets of conditions: (A) the Williams equilibrium (*1*) model with 99% relative humidity in the viscous sublayer, (B) growth according to eq 4 under equilibrium conditions with the Avery (*17*) relative humidity profile, (C) growth according to eq 4 under non-equilibrium conditions with the relative humidity profile used in Williams (*1*) with 99% relative humidity in the viscous sublayer, (D) growth according to the non-equilibrium model presented here (eq 4) with the Avery (*17*) relative humidity profile, (E) no hygroscopic growth. All results presented in this figure are for solid (deliquescing) particles.

these parameters. Model runs were conducted over a range of likely values for the accommodation coefficient, initial relative humidity, temperature, and wind speed. The model was run using the size distribution for $(NH_4)_2SO_4$ as described previously with all combinations of the different values of these parameters. Results are compared to the following base case values: wind speed = 2 m/s, initial relative humidity = 75%, temperature = 20 °C, and accommodation coefficient = 0.1.

The model is most sensitive to large changes in the wind speed, with deposition velocities for wind speeds of 10 m/s up to 1000% higher than the base case. However, smaller changes in the wind speed (U = 0.5−5 m/s) lead to only minor differences in the overall deposition velocity. At very high wind speeds, the height of viscous sublayer is reduced and the turbulence is increased, leading to much greater deposition velocities. At these high wind speeds, hygroscopic growth is relatively unimportant due to the rapid transfer of aerosols to the surface.

When hygroscopic growth is an important consideration, initial relative humidity and temperature have the most significant effects on dry deposition velocity predictions. At a relative humidity of 60%, the deposition velocity is decreased slightly because the relative humidity does not reach the deliquescence point until much closer to the water surface. Although the relative humidity above a water surface may be greater than 80%, this value was chosen as an upper limit because the deliquescence point of $(NH_4)_2SO_4$ is 80.2%. Above the deliquescence humidity, the particles will already be in solution, and the problem is that of metastable droplets, which is examined separately. A relative humidity of 80% leads to increases up to 25% in the deposition velocity because the particles deliquesce further from the water surface and have more time to grow.

The temperature affects the growth and deposition velocity because the diffusivity of water vapor, the viscosity of air, and the deliquescence relative humidity are functions of temperature. An increase in temperature leads to an increase in the diffusivity and viscosity and a decrease in the relative humidity of deliquescence. The increased water vapor diffusivity leads to increased rates of hygroscopic growth as water moves more quickly to the particle surface. An increase in viscosity leads to a decrease in deposition velocity due to decreased air movement. At 5 °C, there is very little deviation from the base case, while a temperature of 35 °C decreases the deposition velocity by up to 21%.

The accommodation coefficient is assumed to equal 0.1 based on the accommodation coefficient for SO_2 (*33*). No data are currently available on the accommodation coefficient of $(NH_4)_2SO_4$. Over a wide range of accommodation coefficients (0.001−1), the deposition velocity does not change significantly.

Acknowledgments

Thanks to V. Etyemezian and W. Dai for many helpful discussions regarding this work. This research was funded by EPA Grant CR 82-2054-01-1 through a subcontract with the University of Michigan and by EPA Grant R-81-9897-01-0.

Literature Cited

(1) Williams, R. M. *Atmos. Environ.* **1982**, *16*, 1933−1938.
(2) Henry, C. D.; Brezonik, P. L.; Edgerton, E. S. In *Atmospheric Pollutants in Natural Waters*; Eisenreich, S. J., Ed.; Ann Arbor Science Publishers, Inc.: Ann Arbor, MI, 1981; pp 199−215.
(3) Thorton, J. D.; Eisenreich, S. J.; Munger, J. W.; Gorham, E. In *Atmospheric Pollutants in Natural Waters;* Eisenreich, S. J., Ed.; Ann Arbor Science Publishers, Inc.: Ann Arbor, MI, 1981; pp 261−284.
(4) Gatz, D. *Water Air Soil Pollut.* **1975**, *5*, 239−251.
(5) Wu, Z. Y.; Han, M.; Lin, Z. C.; Ondov, J. M. *Atmos. Environ.* **1994**, *28*, 1471−1486.
(6) Davidson, C. I.; Wu, Y.-L. In *Acidic precipitation*; Lindberg, S. E., Page, A. L., Norton, S. A., Eds.; Springer-Verlag: New York, 1990; pp 103−216.
(7) Fitzgerald, J. W. *J. Appl. Meteorol.* **1975**, *14*, 1044−1049.
(8) Warneck, P. *Chemistry of the Natural Atmosphere*; Academic Press, Inc.: San Diego, 1988; pp 297, 330−332.
(9) Slinn, S. A.; Slinn, W. G. N. *Atmos. Environ.* **1980**, *14*, 1013−1016.

(10) Slinn, S. A.; Slinn, W. G. N. In *Atmospheric Pollutants in Natural Waters;* Eisenreich, S. J., Ed.; Ann Arbor Science Publishers, Inc.: Ann Arbor, MI, 1981; pp 23−53.
(11) Fletcher, N. H. *The Physics of Rainclouds*; The University Press: London, 1962.
(12) Dulac, F.; Buat-Menard, P.; Ezat, U.; Melki, S.; Bergametti, G. *Tellus*. **1989**, *41B*, 362−378.
(13) Lindfors, V.; Sylvain, M. J.; Danski, J. In *Precipitation scavenging and atmosphere exchange processes, Proceedings, 5th International Conference on Precipitation Scavenging and Atmosphere-Surface Exchange Processes*; Schwartz, S. E., Slinn, W. G. N., Eds.; Hemisphere Publishing Corp.: Richland, WA, 1992; pp 855−866.
(14) Zufall, M. J.; Davidson, C. I. In *Atmospheric Deposition of Contaminants to the Great Lakes and Coastal Waters*; Baker, J., Ed.; SETAC Press: Pensacola, FL, 1997; pp 1−16.
(15) Seinfeld, J. *Atmospheric Chemistry and Physics of Air Pollution*; John Wiley and Sons: New York, 1986; pp 24−26.
(16) Roll, H. U. *Physics of the Marine Atmosphere*; Academic Press: New York, 1965; pp 247−288.
(17) Avery, K. R. *Literature Search for Atmospheric Humidity Profile Models from the Sea Surface to 1000 Meters*; NOAA Technical Memorandum EDS NODC-1; NOAA: Silver Spring, MD, 1972.
(18) Deacon, E. L.; Webb, E. K. In *The Sea: Ideas and Observations*; Hill, M. N., Ed.; Wiley: New York, 1962; Vol. I, pp 43−87.
(19) Montgomery, R. B. *Papers in Physical Oceanography and Meteorology*; Massachusetts Institute of Technology and Woods Hole Oceanographic Institution: Cambridge and Woods Hole, MA, 1940; pp 1−30.
(20) Fuchs, N. A.; Sutugin, A. G. In *Topics in Current Aerosol Research*; Hidy, G. M., Brock, J. R., Eds.; Pergamon Press: New York, 1971.
(21) Pandis, S. N.; Russell, L. M.; Seinfeld, J. H. *J. Geophys. Res.* **1994**, *99*, 16945−16957.
(22) Lowe, P. R.; Ficke, J. M. *Technical Paper No. 4-74*; Environmental Prediction Research Facility, Naval Post Graduate School: Monterey, CA, 1974.
(23) Pruppacher, H. R.; Klett, J. D. *Microphysics of Clouds and Precipitation*; D. Reidel Publishing Co.: Dordecht, 1980; pp 71−99.
(24) Kusik, C. L.; Meissner, H. P. *Ind. Eng. Chem. Process Des. Dev.* **1973**, *12*, 112−115.
(25) Chan, C. K.; Flagan, R. C.; Seinfeld, J. H. *Atmos. Environ.* **1992**, *26A*, 1661−1673.
(26) Tang, I. N.; Munkelwitz, H. R. *Atmos. Environ.* **1993**, *27A*, 467−473.
(27) Pitchford, M. L.; McMurray, P. H. *Atmos Environ.* **1994**, *28*, 827−839.
(28) Rood, M. J.; Shaw, M. A.; Larson, T. V.; Covert, D. S. *Nature* **1989**, *337*, 537−539.
(29) Jenkin, M. E. *Atmos. Environ.* **1984**, *18*, 1017−1024.
(30) John, W.; Wall, S. M.; Ondo, J. L.; Winklmayr, W. *Atmos. Environ.* **1990**, *24A*, 2349−2359.
(31) Milford, J. B.; Davidson, C. I. *J. Air Pollut. Control Assoc.* **1985**, *35*, 1249−1260.
(32) Davidson, C. I.; Jaffrezo, J. L.; Mosher, B.; Dibb, J. E.; Borys, R. D.; Bodhaine, B. A.; Boutron, C. F.; Ducroz, F. M.; Cachier, H.; Ducret, J.; Colin, J. L.; Heidam, N. Z.; Kemp, K.; Hillamo, R. *Atmos. Environ.* **1993**, *27A*, 2709−2722.
(33) Pandis, S. N.; Pilinis, C. In *Airborne Particulate Matter*; Kouitmtzis, T., Samara, C., Eds.; Springer-Verlag: Heidleberg, Germany, 1995; pp 37−67.

Received for review May 29, 1997. Revised manuscript received November 4, 1997. Accepted November 17, 1997.

ES970476R